

## **Changes in NAD and lipid metabolism drive acidosis induced acute kidney injury**

**Milica Bugarski<sup>1</sup>, Susan Ghazi<sup>1</sup>, Marcello Polesel<sup>1</sup>, Joana R Martins<sup>1,2</sup>, Andrew M Hall<sup>1,3</sup>.**

<sup>1</sup>Institute of Anatomy, University of Zurich, Switzerland. <sup>2</sup>Center for Microscopy and Image Analysis, University of Zurich, Switzerland. <sup>3</sup>Department of Nephrology, University Hospital Zurich, Switzerland.

**Supplementary Material**

**Table of contents:**

**Supplementary Figure 1. Effect of pH on NADH fluorescence.**

**Supplementary Figure 2. Identification of proximal tubule segments in kidney slices.**

**Supplementary Figure 3. Acidosis induces the appearance of vacuoles in S2 segments of the proximal tubule.**

**Supplementary Figure 4. Lipidomic analysis (LC-MS) of kidney cortex from mice subjected to water or acid gavage.**

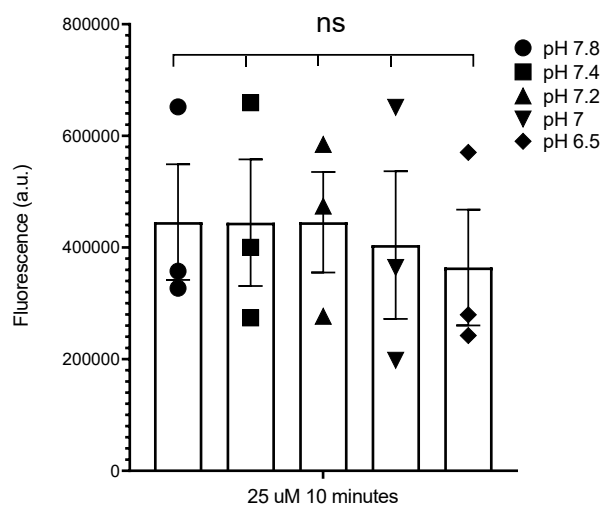
**Supplementary Figure 5. Acidosis-induced damage in proximal tubules.**

**Supplementary Figure 6. Supplementation with NAD induces an acute increase in proximal tubular NAD(P)H signal in kidney slices.**

**Supplemental methods**

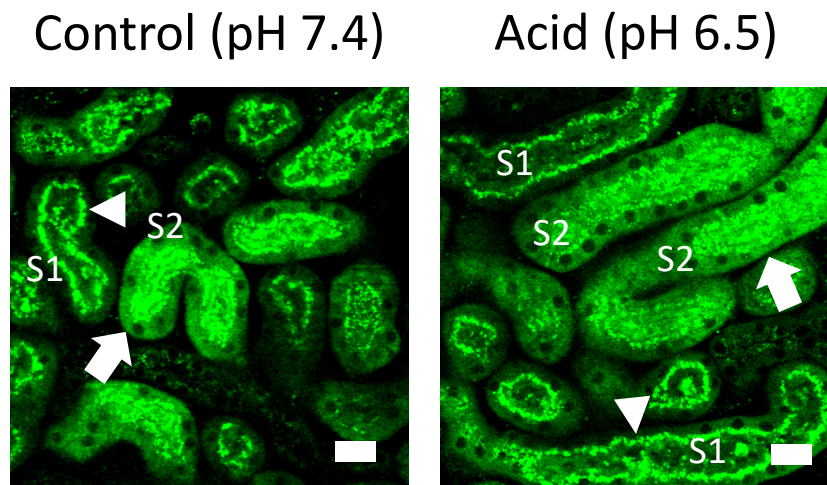
## Supplemental figures

### Supplementary Figure 1



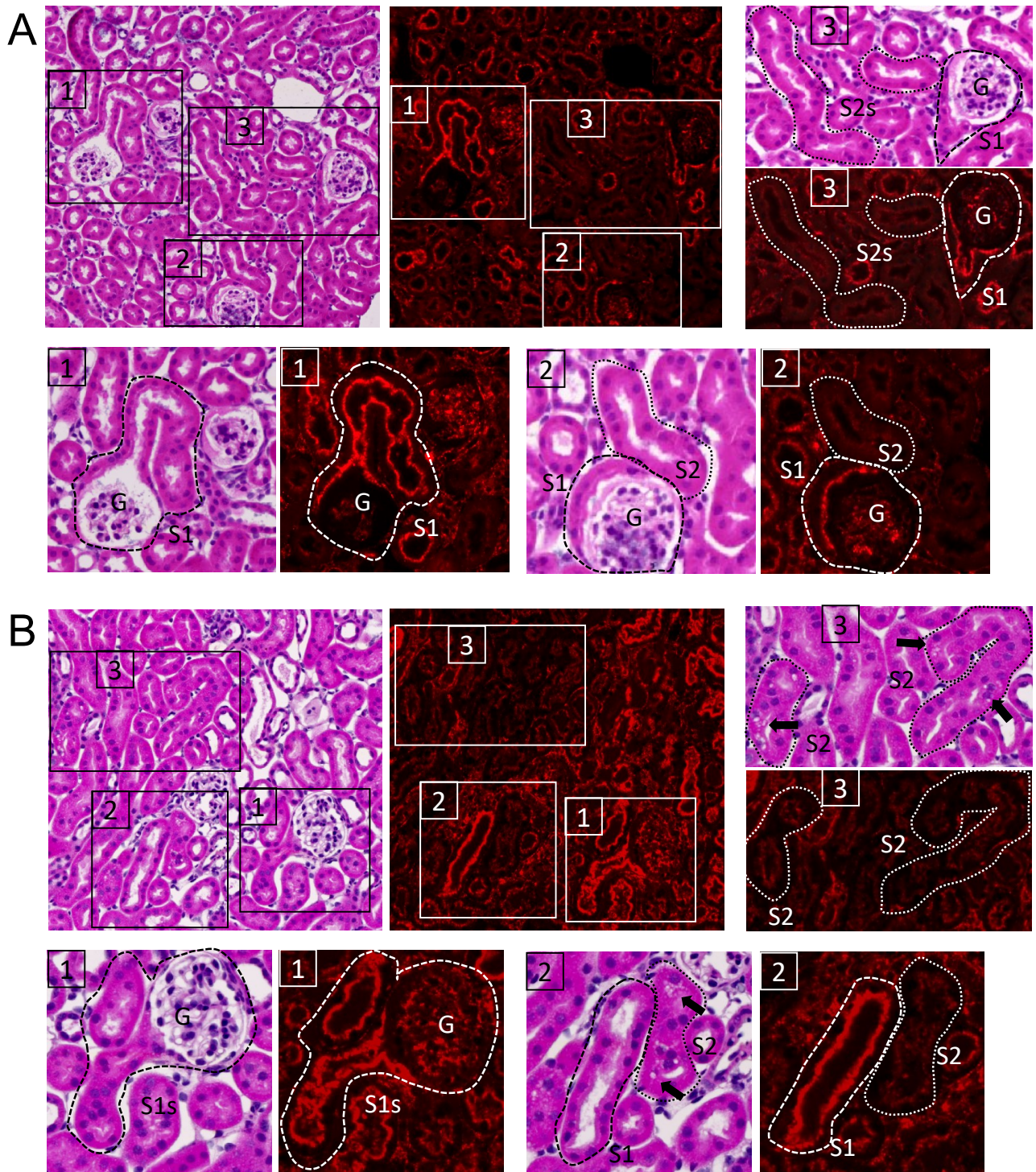
**Supplementary Figure 1. Effect of pH on NADH fluorescence.** NADH (25  $\mu$ M) emission fluorescence (440 – 480 nm) measured in different pH conditions. The values were obtained after excitation at 360 nm at room temperature after 10 minutes. NADH was dissolved in physiological slice buffer.  $n = 3$  wells per plate from 3 different experiments;  $P = 0.9$  for pH 7.8 vs. pH 7.4;  $P = 0.9$  for pH 7.8 vs. pH 7.2;  $P = 0.9$  for pH 7.8 vs pH 7;  $P = 0.9$  for pH 7.8 vs pH 6.5;  $P > 0.9$  for pH 7.4 vs pH 7.2;  $P = 0.9$  for pH 7.4 vs. pH 7;  $P = 0.8$  for pH 7.4 vs. pH 6.5;  $P = 0.9$  for pH 7.2 vs pH 7;  $P = 0.8$  for pH 7.2 vs pH 6.5 and  $P = 0.9$  for pH 7 vs pH 6.5 after 1-way ANOVA - Tukey's multiple comparisons test. a.u., arbitrary units.

Supplementary Figure 2



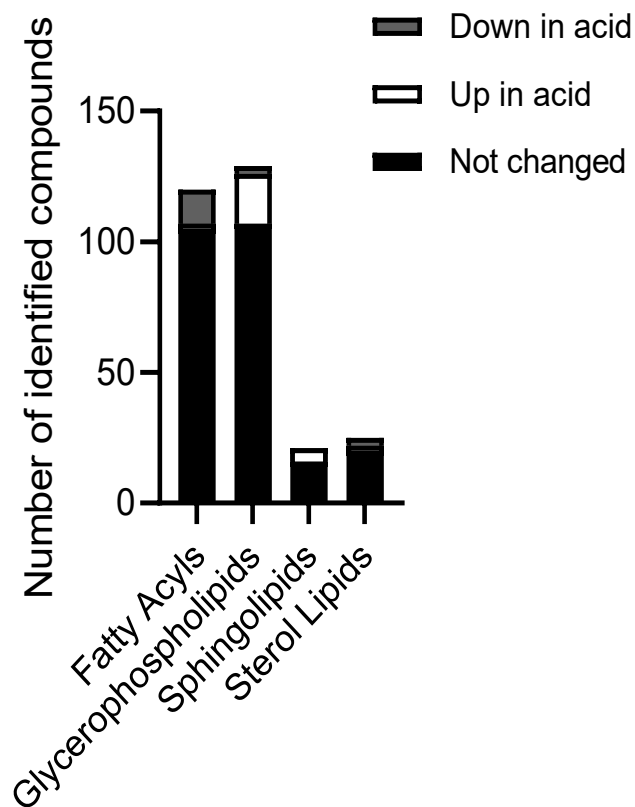
**Supplementary Figure 2. Identification of proximal tubule segments in kidney slices.** Autofluorescence signal excited at 900 nm in cortical kidney slices revealed higher mitochondrial flavoprotein fluorescence (arrows) in S2 proximal tubules (PT), whilst S1s showed bright vesicular signal in the sub-apical region (arrowheads) originating from the endolysosomal system. These fluorescent characteristics were observed under both control and acid conditions. Scale bars = 20  $\mu$ m. S1 segment of the PT; S2, S2 segment of the PT.

Supplementary Figure 3



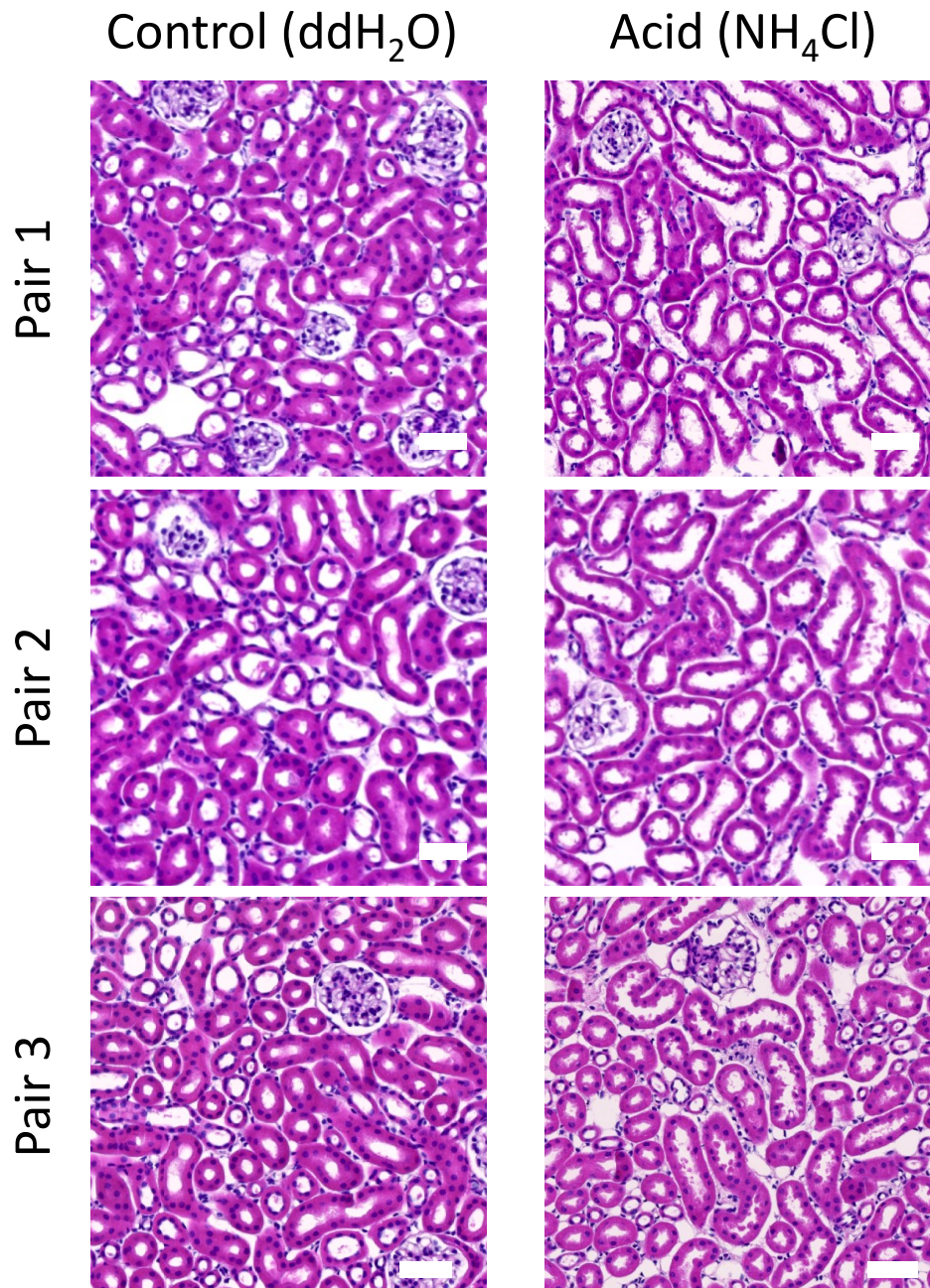
**Supplementary Figure 3. Acidosis induces the appearance of vacuoles in S2 segments of the proximal tubule.** Haematoxylin and eosin (H&E) and LAMP1 antibody staining in **A**) control - and **B**) acid - treated mice. S1 proximal tubules (PTs) were identified as directly emerging out of the glomerulus (G) (**A 1-3**), whereas a second population of PTs with low LAMP1 signal were identified as S2s (**A 2-3**). In acid-treated animals, S1 PTs showed no vacuole formation (**B 1-2**), whilst vacuoles (arrows) appeared in low LAMP1 signal S2 PT segments (**B 2-3**). Scale bars = 20  $\mu$ m. G, glomerulus; S1, S1 segment of the PT; S2, S2 segment of the PT.

Supplementary Figure 4



**Supplementary Figure 4. Lipidomic analysis (LC-MS) of kidney cortex from mice subjected to water or acid gavage.** Lipid levels were measured 2.5 hours after gavage and classified according to type. Data depicted show the number of identified lipids per category with a significant change ( $p < 0.05$ ) in abundance between the two groups.

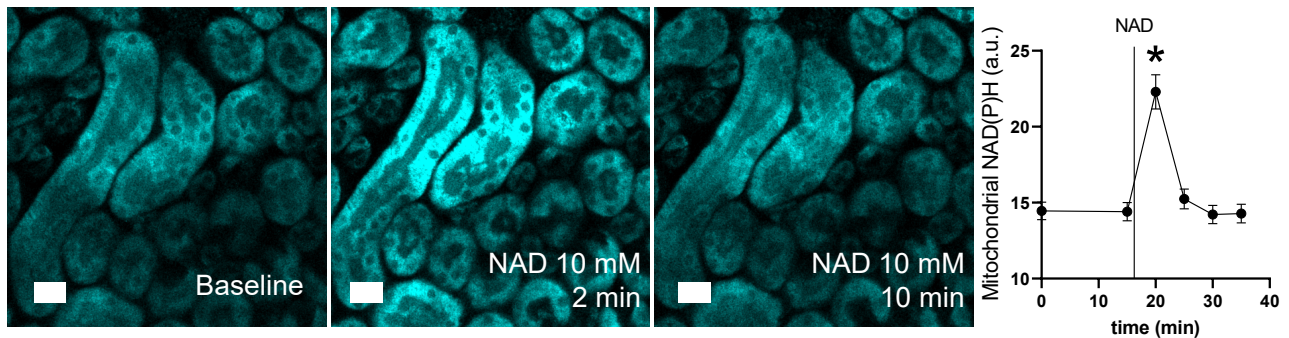
Supplementary Figure 5



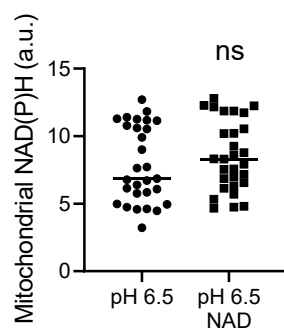
**Supplementary Figure 5. Acidosis-induced damage in proximal tubules.** Representative overview images of Haematoxylin and eosin (H&E) stained kidney tissue from water- and acid-fed mice 3 hours post-gavage. Proximal tubular damage – including dilatation and thinning of tubules and apical shedding of cellular debris - was only observed in acid-treated animals. Scale bars = 50  $\mu$ m.

## Supplementary Figure 6

### A



### B



**Supplementary Figure 6. Supplementation with NAD induces an acute increase in proximal tubular NAD(P)H signal in kidney slices.** **A)** Addition of NAD (10 mM) triggered a transient rise in mitochondrial NAD(P)H signal in the proximal tubule (PT), after which new equilibrium was reached ( $n = 11$  tubules from 3 different slices from 3 different animals).  $P < 0.0001$  for baseline vs NAD after paired t-test. **B)** NAD(P)H signal in PTs was not significantly changed following incubation of kidney slices for one hour at pH 6.5 with 10 mM NAD, when compared to slices exposed to acid alone ( $n = 29$  PTs from 4 different slices from 4 different animals).  $P = 0.38$  for pH 6.5 vs. pH 6.5 NAD after unpaired t-test. Scale bars = 20  $\mu\text{m}$ . a.u., arbitrary units.

## **Supplemental methods**

### ***Effect of pH on NADH fluorescence in solution***

$\beta$ -Nicotinamide adenine dinucleotide, reduced disodium salt hydrate (Sigma Aldrich), was dissolved (25  $\mu$ M) in physiological slice buffer, containing (in mM): 118 NaCl, 4.7 KCl, 1.2  $\text{KH}_2\text{PO}_4$ , 1.8  $\text{CaCl}_2$ , 1.44  $\text{MgSO}_4$ , 5 glucose, 10  $\text{NaHCO}_3$ , 10 HEPES, 5 sodium pyruvate, 2.5 sodium butyrate and 2.5 sodium lactate. Slice buffer solutions were titrated to various pH values with 0.1 % HCl or 0.1 % NaOH. The fluorescence emission (420 nm – 460 nm) of NADH was measured in 96 Well Black/Clear Bottom Plate (Thermo Fisher) on a 96-well microplate reader (Biotek GmbH, Sursee, Switzerland). Each experiment was performed in triplicates.

### ***Imaging of kidney slices***

After isolation, the kidney was mounted and cut into 250  $\mu$ m thick sections (Microm HM 650 V, Thermo Scientific, Waltham, Massachusetts, USA). The tissue was kept until usage at 4°C in a physiological slice buffer adjusted to pH 7.4 and gassed with carbogen (95 %  $\text{O}_2$  / 5 %  $\text{CO}_2$ ). Slices were equilibrated in the slice chamber at 37 °C for 30 minutes before NAD (10 mM) was applied in the slice buffer. Slices were pre-incubated in pH 7.4 buffer containing 10 mM NAD for 30 min, before being transferred to pH 6.5 for 1 h incubation. Recordings were performed with an Olympus Fluoview 1000 MPE equipped with an XPlan N 25x/1.05 objective and a ultrafast Ti:Sapphire laser system. NAD(P)H was excited at 720 nm and visualized at 420-500 nm. Green autofluorescence signals were excited at 900 nm and visualized at 515–560 nm.

### ***Histological and immunofluorescence staining***

PFA-fixed, paraffin-embedded blocks were sectioned at 4  $\mu\text{m}$ . Paraffin sections were then dewaxed and rehydrated, and H&E or immunofluorescence staining was performed. For immunofluorescence staining, after permeabilization with 0.1 % TritonX-100 (Surfact-Amps detergent solution; Thermo Fisher Scientific) for 5 minutes, tissue sections were blocked with 1 % BSA and 10 % goat serum before incubation overnight at 4°C with rat monoclonal anti-LAMP1 (ab25245, Abcam, Cambridge, UK, 1:100). After washing with PBS, sections were incubated at room temperature for 2 hours with goat anti-rat-Cy5 antibody (112-607-003, Jackson ImmunoResearch Europe Ltd, Cambridgeshire, UK, 1:500). Slices were mounted with Dako mounting medium (Agilent, Santa Clara, California, USA). Consecutive sections of H&E and LAMP1 were visualized on an Axio Scan.Z1 slidescanner using a Plan Aplanachromat 40x/0.95 air immersion objective.

#### ***Lipidomic (LC-MS) analysis***

After the removal of kidneys, cortex was cut out and frozen immediately in liquid nitrogen. The frozen kidney tissue was weighed and 300  $\mu\text{L}$  of extraction solvent (butanol:methanol:water [9:9:2]) was added and the tissue homogenized with DWK Life Sciences Kimbl BioMasherII Closed System Micro Tissue Homogenizer (Fisher Scientific). The weight range of extracted tissue was between 11 mg and 17 mg. Samples were centrifuged at 14000 g for 20 min at 25 °C. Samples were normalized based on initial tissue weight with extraction solvent resulting in 36.6 mg tissue per mL. Lipids were separated on a nanoAcquity UPLC (Waters) equipped with a HSS T3 capillary column (150  $\mu\text{m}$  x30mm, 1.8  $\mu\text{m}$  particle size, Waters), applying a gradient of 5 mM ammonium acetate in water/acetonitrile 95:5 (A) and 5 mM ammonium acetate in isopropanol/acetonitrile 90:10 (B) from 5% B to 100% B over 10 min. The following 5 min conditions were kept at 100% B, followed by 5 min reequilibration to 5% B. The injection volume was 1  $\mu\text{L}$ . The flow rate was constant at 2.5  $\mu\text{L}/\text{min}$ . The UPLC

was coupled to QExactive mass spectrometer (Thermo) by a nanoESI source. MS data was acquired using positive polarization and data-dependent acquisition (DDA). Full scan MS spectra were acquired in profile mode from 107-1600 m/z with an automatic gain control target of  $1e6$ , an Orbitrap resolution of  $70\ 000$ , and a maximum injection time of 200 ms. The 5 most intense charged ( $z = +1$  or  $+2$ ) precursor ions from each full scan were selected for collision induced dissociation fragmentation. Precursor was accumulated with an isolation window of 0.4 Da, an automatic gain control value of  $5e4$ , a resolution of  $17\ 500$ , a maximum injection time of 50 ms and fragmented with a normalized collision energy of 10, 20 and 30 (arbitrary unit). Generated fragment ions were scanned in the linear trap. Minimal signal intensity for MS2 selection was set to  $5e3$  using as apex trigger (1 to 3 s).

### ***Data processing***

Lipid data sets were evaluated with Progenesis QI software (Nonlinear Dynamics), which aligns the ion intensity maps based on a reference data set, followed by a peak picking on an aggregated ion intensity map. Detected ions were identified based on accurate mass, detected adduct patterns, isotope patterns and theoretical fragmentation by comparing with entries in the LIPID MAPS Data Base (LM). A mass accuracy tolerance of 5 ppm was set for the searches.

Further statistical and enrichments analysis were calculated in Microsoft Excel. An arbitrary detector abundance cutoff of  $10\ 000$  were applied to remove noise. P-values between the groups (4 biological replicates each) were calculated with t-test function (two-tailed, homoscedastic). Compounds with p-values below 0.05 were defined as significant changed. Putative identifications had to fulfill the following prerequisites: mass error (observed mass – exact mass) below 5 ppm, MS2 fragmentation score (Progenesis QI) larger than 5, isotopic similarity larger than 80 %. The remaining putative identifications were ranked by the Progenesis QI overall score. The highest scored identification was assigned to each compound.

LIPID MAPS main class and category for each identified compound were assigned. For enrichment analysis, significant changed compounds (summarized in main class and category) were compared to the background list, consisting of all putative identifications independently of their p-values.

### *Statistics*

Data are presented as mean values ( $\pm$  SEM). All data were analyzed using GraphPad Prism software. Paired and unpaired Student's t tests were used to compare two groups. 1-way ANOVA with Tukey's multiple comparison test was used to compare more than 2 different groups. P values of less than 0.05 were considered statistically significant.